ISSN : 2321-9602

Indo-American Journal of Agricultural and Veterinary Sciences




editor@iajavs.com
iajavs.editor@gmail.com

Indo-American Journal of Agricultural and Veterinary Sciences

ISSN 2321–9602 www.iajavs.com

Three-Phase Solar PV System with Integrated Uninterruptible Power Supply and Battery Energy Storage System Performance Evaluation

T.PRAVEEN[1], MANEESH KUMAR[2]

Abstract:

In order to address grid harmonics and power quality issues, this study investigates the potential of a Unified Power Quality Conditioner (UPQC). In this configuration, the UPQC is backed up by a hybrid renewable energy system consisting of solar panels and batteries. A PV system can often provide all of the active electricity required by the load. If the PV is unable to provide the energy, particularly during the longer-term voltage disruption, the BESS will take over. Because of the greater robustness and immunity to fluctuations and other external effects of a hybrid PV-BESS system, it is more trustworthy than a stand-alone PV-UPQC system. So, BESS will keep producing clean energy while increasing its long-term voltage support capabilities and optimizing the DC-link voltage control algorithm. A Self-Tuning filter (STF) in combination with the unit vector generator (UVG) technology guides the UPQC controller's phase synchronization procedure. Even if the grid voltage is unstable, the UPQC will function well if STF is used. By employing the STF-UVG, the UPQC controller's series and shunt active power filter (APF) compensator may be synced without resorting to a PLL. Finally, the advantages of the new STF-UVG method are shown by contrasting it with the standard UPQC based on the SRF-PLL method. Additional MATLAB-Simulink examples are evaluated for reliability.Battery Energy Storage System (BESS), Self-Tuning Filter (STF), Unified Power Quality Conditioner (UPQC), and Photovoltaics (PV)

I.INTRODUCTION

The source of all life is energy. Among the many types of energy, electricity is a major one. The needfor this kind of energy, which guarantees the adaptability of human existence, is skyrocketing. Recently, scholars have shown an extraordinary amount of interest in the concept of "Power Quality," particularly those working in the field of electrical engineering. To preserve energy efficiency and promote decarbonization of the

1.Assistant professor, Department of Pharmaceutical Analysis, Sri Venkateswara College of Pharmacy, Etcherla, Srikakulam.
2. Assistant professor, Department of Pharmacology, Sri Venkateswara College of pharmacy, Etcherla, Srikakulam.

Indo-American Journal of Agricultural and Veterinary Sciences
ISSN 2321–9602 www.iajavs.com

system, power quality concerns are offset by adjusting for them. Power quality is a fluidmeaning that may take on a variety of connotations and applications depending on the specific context. For instance, the utility is worried about the network being impacted by harmonics produced by non-linear loads, while customers are worried about disruptions in the provided voltage. Interference in neighboring communication lines and interruption for various customers may result from power losses and the undesired and abnormal features of equipment brought on by power quality issues. IEEE-1159 [1] defined the characteristics of a reference waveform and classified various types of noise. For example, fluctuation or harmonics for a brief time distortion like sags or surges, together make up a complicated power quality scenario [2]. When sensitive loads, for example, trip due to voltage disturbances such voltage harmonics, voltage swells, and voltage sags, it may have serious repercussions for manufacturing facilities, such as the cessation of production.

The industry is used to these kinds of situations, which result in significant financial losses. In order to protect their facilities against grid-sourced disruptions, industrial clients have begun installing mitigation devices from the series APFs [3]-[8]. Shunt active power filters (APFs) are used to mitigate problems caused by the proliferation of power electronics in contemporary power plants, such as harmonics production and sensitive load in the system [9]- [12]. As a result, a new norm has emerged that serves the utility's needs while also meeting the demands of its patrons. The importance of this trend lies in the fact that it protects both the utility and the consumers at the same time, shielding the delicate components from voltage fluctuations and reducing the amount of distortion introduced to the utility by the loads being used by the latter [13]. With a series and shunt APF compensator in a

Indo-American Journal of Agricultural and Veterinary Sciences

ISSN 2321–9602 www.iajavs.com

back-to-back arrangement, the UPQC model hasthe ability to regulate the load voltage and the grid current simultaneously [14]. The growingpopularity of microgrids and decentralized power plants has piqued academics' interest in UPQC [15– 17]. Additionally, there has been a rise in concern about the usage of renewable power sources, with the aim of decreasing reliance on the rapidly dwindling supply of fossil fuels that contribute to both global warming and its cause. Renewable energy solutions are essential because they improveelectricity quality and can keep running even if the grid goes down. In [19], the authors suggested integrating a fuel cell (FC) with UPQC to successfully alleviate PQ concerns on the grid side by providing actual power supply during voltage interruption. However, they have neither promoted decarbonization of the grid-connected system or emphasized the integration of renewable energy resources with UPQC in their research. [20]presented a PV integrated with UPQC to solve boththe power quality issues and the need for sustainable energy. But they didn't account for protracted interruptions or significant power drops. Meanwhile, the problem of prolonged outages was solved by coupling a dynamic voltage restorer (DVR) with a superconducting magnetic energy storage system (SMES) to sustain the load. However, the issue of associated harmonics in the present tense was overlooked. A BESS or similar energy storage system interfaced with the PVUPQC would be an excellent back-up for supplying steady, usable power to the load. For renewable energy systems, BESS is especially important when the UPQC is running independently. When used to important loads like semiconductor factories, hospitals, and data centers, where a constant supply of high-quality electricity is essential, the BESS's higher price tag becomes understandable. As a result, the PV and BESS were designed to support the UPQC. Both the photovoltaic array and the battery energy storage system (BESS) are linked to the DC-link, one through a DC-DC boost converter and the othervia a DC-DC buck-boost converter. When the PV system is unable to deliver the active power to the load, the BESS kicks in and does so, particularly during the longer-term voltage interruption, to improve distribution power system reliability. It is the goal of the study presented in [19] to develop an algorithm for regulating the voltage across the DC link, which would keep the voltage across the DC link capacitor constant and steady. However, the computational complexity and load of the UPQC controller continue to rise. PV-BESS, on theother hand, may be preferable because of its ability to externally support the DC-link capacitor of aUPQC, hence reducing the DC-link capacitor's workload. An UPQC system's synchronizationphase is crucial to its overall operation. It is important to keep in mind that the shunt APF compensator and the series APF compensator both rely on precise synchronization phase operation to provide the reference current and voltage, respectively [28]. Injecting voltage and current in phase with the grid is essential for the UPQC to successfully complete the synchronization procedure. Most UPQC controllers in [15] rely on an old-school SRF-PLL for the synchronization phase algorithm, making them helpless against voltage distortion and imbalance. Additionally, the low pass filter used in a standard PLL controller's synchronization process results in unwanted ripplesin the reference current and voltage. Another drawback of PLLs is that their PI controllers make fine tuning more difficult and time consuming. Using STF with improved phase tracking and fundamental component extraction might help with synchronizing phase detection. The extraction ofthe harmonic current algorithm and the voltage error algorithm both need the formation of unit vectors consisting of the sine and cosine function; this work's goal is to develop a simple controller structure based on this idea. In addition, the phases of synchronization are applied to the reference current generation in a shunt compensator that is designed with integrating together with a strong STF based on the direct-quadrature-zero (STF-dq0)concept of operation and does not rely on any components of a phase-locked loop (PLL). The reference voltage generation in a seriescompensator will make use of synchronization phases to provide in-phase compensation, employing the same operating principle as the dq0. When dealing with an imbalanced and distorted voltage grid, the recommended approach that will be applied to the UPQC controller must prove to bebetter and more trustworthy. Maintaining a sinusoidal grid current by controlling the target load voltage and limiting the phase difference to approach unity power factor is another capability.

In this study, we suggest a parallel connection of PV and BESS with UPQC as a means of addressingthe complicated power quality issues that arise, in

Indo-American Journal of Agricultural and Veterinary Sciences

ISSN 2321–9602 www.iajavs.com

particular during prolonged voltage interruptions. The proposed UPQC is integrated with PV and BESS, and its dynamic performance is verified using a number of case studies. There is also acomparison between the efficiency of UPQCs that simply use a DC-link capacitor and those that include use PV and BESS. In addition, the synchronization phases for the UPQC controller are generated using the STF combined with the UVG technology (STF-UVG) to overcome the shortcomings of the traditional PLL. To demonstrate the advantages of the suggested method, we compare the STF-performance UVG's to that of a regular SRF-PLL. Lastly, MATLAB-Simulink is used to examine the proposed UPQC system's functionality in a dynamic setting.

II. PROPOSED SYTEM

In Fig.1 we can see how the PV-BESS-UPQC was put together. The PV-BESS-UPQC model is intended for use with the three-phase system. The PV-BESS-UPQC is made up of a series and shunt APF compensator coupled with a DC-link split capacitor. The DC-link is paralleled with the connections between the battery and PV array. By means of a boost converter, the PV is connected to the DC-link. As an added bonus, a buck-boost converter connects the BESS to the DC-link. The supply voltage sags, swells, interruption, and voltage harmonics are all alleviated by the series compensator, which operates as a regulated voltage source. The shunt compensator, on the other hand, reduces the load current's harmonics. Inductors serve as connectors between the series and shunt APF compensators. Since harmonics are created by the converter's switching activity, a ripple filter is used to remove them. The series compensator injects power into the grid using a series injection transformer. Three-phase non-linear loading is used in this investigation. Precision measurements of the PV array, split capacitor, reference voltage of DC-link, etc., are the first step in the PV-BESS-UPQC design process. The shunt compensator was created in such a manner that, in addition to reducing current harmonics, it limits the maximum power that can be generated by the PV array. The PV array's maximum power point (MPP) voltage is equal to the reference DC-link voltage because of the PV array's direct connection to the UPQC DC- link. In normal operating circumstances, the PV array's rating guarantees that it will supply the grid and charge the BESS, as well as provide the active power needed to run the load. When the PV array's output is less than the DC-link load demand, the BESS steps in to make up the difference by supplying electricity at a lower voltage to the DC-link. In addition, the BESS will meet the whole demand load if the PV array is not producing any electricity.

Since harmonics are created by the converter's switching activity, a ripple filter is used to remove them. The series compensator injects power into the grid using a series injection transformer. Three-phase non-linear loading is used in this investigation. Precision measurements of the PV array, split capacitor, reference voltage of DC-link, etc., are the first step in the PV-BESS-UPQC design process. The shunt compensator was createdin such a manner that, in addition to reducing current harmonics, it limits the maximum power that can be generated by the PV array. The PV array's maximum power point (MPP) voltage is equal to the reference DC-link voltage because of the PV array's direct connection to the UPQC DC- link. The active power required to run the load is met by the PV array under normal circumstances, and the array also provides electricity to the gridand charges the BESS. When the PV array produces less power than the DC-link load requirement, the BESS supplies the missing power, offsetting the drop in DC-link voltage. In addition, the BESS will meet the full demand load when the PV array is not producing any electricity.

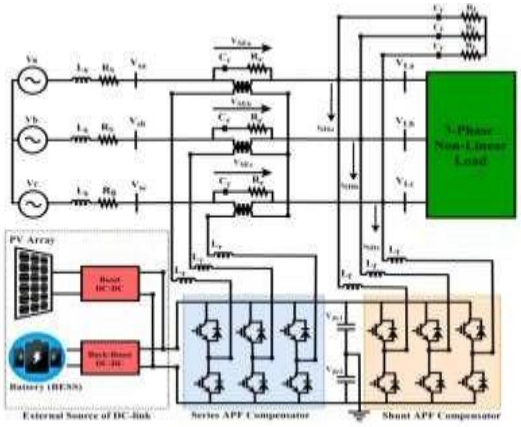

Figure. 1. UPQC system configuration

DESIGN OF UPQC CONNECTING WITH PV-BESS AS EXTERNAL SUPPORT OF DC-LINK

The PV system, BESS, boost converter, buck-boost converters, and controller are all part of the

Indo-American Journal of Agricultural and Veterinary Sciences

ISSN 2321–9602 www.iajavs.com

recommended model shown in Fig. 2. By connecting the BESS with a buck-boost converterin parallel with the DC-link capacitor, the UPQC's stability is enhanced, allowing it to better compensate for power quality issues. The entirepower flow in the model is denoted by (7). In addition, Table 1 lists the specifications of the PV system and the parameters of the Li-ion batterysystem used in this research.

$$P_{total} = P_{pv} + P_{BESS} - P_{Load_{DC-link}}$$

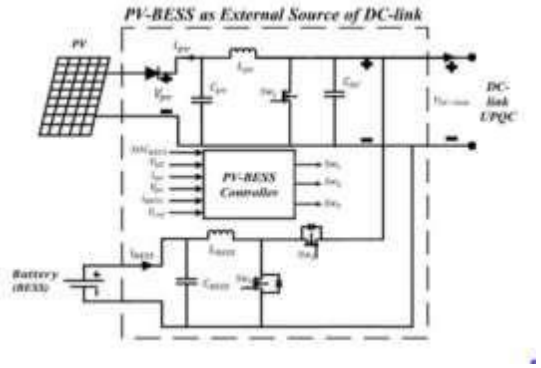

Fig. 2. PV-BESS system configuration

TABLE. 1. Parameters of devices implemented in the work

Device	Parameters	Values
PV panel single panel (SunPower SPR-215-WHT-U)	Rated Power	214.92 W
	Open circuit voltage (V_{oc})	48.3 V
	Short circuit current (I_{sc})	5.8 A
	Voltage at maximum power (V_{mp})	39.8 V
	Current at maximum power (I_{mp})	5.4 A
	Number of cells in parallel	11
	Number of cells in series	18
	Temperature	25 ◦C
Li-ion battery	Rated Capacity	350 Ah
	Maximum Capacity	450 Ah
	Nominal voltage	650 V
	Fully charge voltage	756 V

PV system model

An example of a popular kind of PV module design, the single diode model is shown in Figure 6.3.

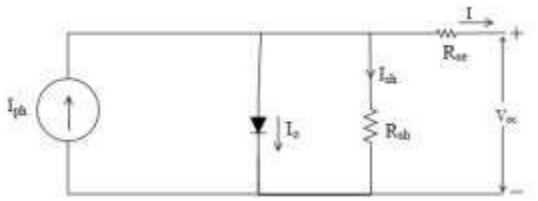

Fig.3 Solar cell equivalent circuit

KCL is used in this circuit to get the cell current expression for the single diode model.

$$I = Iph - Io - Ish \quad (1)$$

$$\text{Where, } Iph = [Isc + Ki\,(Tk - T)] * G/1000$$

Standard test circumstances (STC), with reference solar radiation of 1000 W/m2 at solar spectrum of 1.5A and reference temperature of solar cell Tk of 25°C, provide a photocurrent denoted by Iph. Here, T is the instantaneous temperature of the solar cell, Ki is the instantaneous temperature coefficient, and G is the instantaneous solar radiation.

Current Saturation Module in Reverse (Irs)

The Irs value for the reverse saturation current of a module is:

$$Irs = Isc/\,[\exp\,(q * Voc/Ns * k * A * T) - 1] \quad (2)$$

Where q is the charge on an electron (1.6 x 1019 C), Voc is the open-circuit voltage of the solarmodule, Ns is the number of series-connected cells,and A is the ideality factor (A=1.6). to which we add the Boltzmann constant, k (k= 1.3805 1023 J/K).

Saturation Current (I0) in a Module The saturation current in a module varies as a function of cell temperature. A formal representation of this idea is as follows:

Irs=I0 [T/Tr] There is a threefold exponentiation of [q*Eg0/Ak*(1/Tr)-(1/T)] (3)

The band gap energy of a semiconductor is denoted by Eg0.

It has been simulated what happens when you plug (3) into a computer. Module operating temperature, reference temperature, and reverse saturation current are the inputs here.

Indo-American Journal of Agricultural and Veterinary Sciences

ISSN 2321–9602 www.iajavs.com

Current Output From A Module (IPV)

A simple equation may be used to explain the current drawn from a PV module's output diode, as shown in Figure 3: Ipv=Np*Iph-Np*I0. "[exp q*(Vpv+Ipv*Rse)*Ns*A*k*T1]" (4)

To preserve the MPPT algorithm, the duty cycle of the DC-DC boost converter must be controlled. In this study, we use a straightforward technique called Perturb and observe (P & O) since it provides the most precise tracking of the MPP. The MPPT algorithm takes as input the voltage and current produced by the PV module (shown by the flowchart in Fig. 4). In order to put this procedure into action, it is necessary to first measure the current and voltage of PV modules in order to calculate the power of PV modules, Ppv. Continuous monitoring and small adjustments are made until the operating point reaches the maximum practical point. When estimating how long it will take to attain MPP, the algorithm compares the voltages and powers over time (n) to a sample taken over time (n 1). With the MPPT of the PV module, the P & O algorithm monitors by routinely raising or decreasing voltage. When a positive power shift happens, even a little voltage change may affect the output of the solar panels, and the voltage change tends to stay on the same trajectory. When the delta power is negative, on the other hand, it indicates that the MPP is faraway and that the perturbation must be attenuated before it can be reached. Table 2 provides a brief overview of the P & O algorithm.

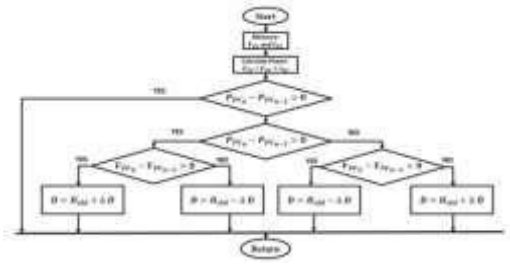

Fig. 4 Algorithm Flowchart for "Disturb and Observe"

The Perturb&Observe algorithm's structure is shown in Table.2.

Perturbation	ΔP	Perturbation Output
+ve	+ve	+ve
+ve	−ve	−ve
−ve	+ve	−ve
−ve	−ve	+ve

BATTERY ENERGY STORAGE SYSTEM MODELLING

To attain the required nominal voltage and capacity for the BESS modeling, batteries typically consist of many electrochemical cells connected in series and/or parallel. The electrochemical model and the electric circuit model provide the basis for the categorization of battery models, and the other models are often derived from these two. By integrating current, for instance using Peukert's equation, we may create a more accurate model of a battery. In addition, the electrochemical model known as Stepherd's equation. Mathematical modeling is used because of powerful software like SIMULINK/MATLAB. Given its superiority over other batteries in terms of power density, energy capacity, rate of self-discharge, and cost of maintenance, the Li-ion battery was chosen for this project. All of the values for the BESS system's parameters that were calculated for this study are included in Table.3.

Fig. 6.5 depicts the internal and exterior control loops of the bidirectional converter Buck-Boost DC-DC controller in charging and discharging mode.

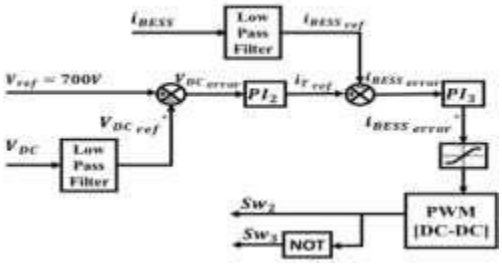

Fig. 5 Scheme for Controlling the BESS's DC-DC Buck-Boost Converter

III. WORKING PRINCIPLE OF THE PROPOSED CONTROL OF PV-BESS-UPQC USING SELF-TUNING FILTER TECHNIQUE

STF-UVG SYNCHRONIZATION TECHNIQUE

The suggested STF-UVG methodology is non-iterative and uses a simple way to extract the synchronization phases from the supply voltage.The STF method used in the UPQC controller system is seen in Fig. 6. As shown in (5), the three-phase supply voltage exists in matrix form, and the Clarke transformation matrix is used to transfer thevoltage from the abc-domain to the 0-domain.

Indo-American Journal of Agricultural and Veterinary Sciences

ISSN 2321–9602 www.iajavs.com

$$\begin{bmatrix} V_{S_\alpha} \\ V_{S_\beta} \\ V_{S_o} \end{bmatrix} = \sqrt{\frac{2}{3}} \begin{bmatrix} 1 & -\frac{1}{2} & -\frac{1}{2} \\ 0 & \frac{\sqrt{3}}{2} & -\frac{\sqrt{3}}{2} \\ \frac{1}{2} & \frac{1}{2} & \frac{1}{2} \end{bmatrix} \begin{bmatrix} V_a \\ V_b \\ V_c \end{bmatrix} \quad (5)$$

When just two phases are taken into account in the -domain, the distorted supply voltage may be decomposed into its fundamental and harmonic components. This connection is shown by (6)

$$\begin{bmatrix} V_{S_\alpha} \\ V_{S_\beta} \end{bmatrix} = \begin{bmatrix} V_{S_{\alpha\,(fund)}} + V_{S_{\alpha(har)}} \\ V_{S_{\beta\,(fund)}} + V_{S_{\beta(har)}} \end{bmatrix} \quad (6)$$

The fundamental (fund) component is denoted by Vs,(fund), whereas the harmonic (har) component is denoted by Vs,(har) in the - domain. The generation of synchronization phases calls on both of the basic -domain components. Using the self- tuning filtering (STF) technique, the core elements are isolated. Existing harmonic components in the distorted supply voltage are muted using the STF technique. Since this is the case, the derived synchronization phases are more accurate and of higher quality. A typical STF transfer function is expressed after performing the Laplace transformation.

$$\begin{bmatrix} V_{S_{\alpha\,(fund)}}(s) \\ V_{S_{\beta\,(fund)}}(s) \end{bmatrix} = \frac{K_1}{s} \begin{bmatrix} V_{S_\alpha}(s) - V_{S_{\alpha\,(fund)}}(s) \\ V_{S_\beta}(s) - V_{S_{\beta\,(fund)}}(s) \end{bmatrix} + \frac{2\pi f_{c1}}{s} \begin{bmatrix} -V_{S_{\beta\,(fund)}}(s) \\ V_{S_{\alpha\,(fund)}}(s) \end{bmatrix} \quad (7)$$

The cutoff frequency, fc1, is shown above, and the constant gain parameter, K1, is the gain at that frequency. K1's rating is roughly between 20 and 80, whereas fc1's rating is proportional to the system's frequency. The anticipated K1 rating for this project is 20, and the fc1 rating is 50 Hz. It is shown in that if Vs,(fund) and Vs,(fund) are available, then the sin(t) and cos(t) synchronization phases may be obtained.

$$\begin{bmatrix} \sin(\omega t) \\ \cos(\omega t) \end{bmatrix} = \frac{1}{\sqrt{(V_{S_{\alpha\,(fund)}})^2 + (V_{S_{\beta\,(fund)}})^2}} \begin{bmatrix} V_{S_{\alpha\,(fund)}} \\ -V_{S_{\beta\,(fund)}} \end{bmatrix} \quad (8)$$

Synchronization phases may be successfully generated in the presence of supply voltage distortion in UPQC by using (8) as UVG approach, thereby eliminating the need for a typical PLL element.

MODIFICATIONS TO THE SERIES APF COMPENSATION PLAN

Using the phase and frequency information from STF-UVG, we can get the abc-domain value for the three-phase reference voltage signal, Vref,abc, as shown in (9) below. In this case, the amplitude at its peak of the voltage that supplies the load (the fundamental voltage) is used to calculate the maximum peak voltage magnitude, Vm,maxpeak. At PCC, the reference voltage signal should be in phase with the supply voltage, with the d-frames components being the peak amplitude of the load reference voltage and the q-frames components being set to zero.

$$\begin{bmatrix} V_{ref_a}{}^* \\ V_{ref_b}{}^* \\ V_{ref_c}{}^* \end{bmatrix} = V_{m_{max-peak}} \begin{bmatrix} \sin(\omega t) \\ \sin(\omega t - \frac{2\pi}{3}) \\ \sin(\omega t + \frac{2\pi}{3}) \end{bmatrix} \quad (9)$$

$$\begin{bmatrix} V_{ref_\alpha}{}^* \\ V_{ref_\beta}{}^* \\ V_{ref_o}{}^* \end{bmatrix} = \sqrt{\frac{2}{3}} \begin{bmatrix} 1 & -\frac{1}{2} & -\frac{1}{2} \\ 0 & \frac{\sqrt{3}}{2} & -\frac{\sqrt{3}}{2} \\ \frac{1}{2} & \frac{1}{2} & \frac{1}{2} \end{bmatrix} \begin{bmatrix} V_{ref_a}{}^* \\ V_{ref_b}{}^* \\ V_{ref_c}{}^* \end{bmatrix} \quad 10)$$

$$\begin{bmatrix} V_{ref_d}{}^* \\ V_{ref_q}{}^* \end{bmatrix} = \begin{bmatrix} \cos(\omega t) & \sin(\omega t) \\ -\sin(\omega t) & \cos(\omega t) \end{bmatrix} \begin{bmatrix} V_{ref_\alpha}{}^* \\ V_{ref_\beta}{}^* \end{bmatrix} \quad (11)$$

The reference voltage signal is transformed from the abc domain to the 0-domain using the Clarke transformation matrix and the three-phase reference voltage signal shown in matrix form in (12). Then, the suggested STF-UVG is used to extract the fundamental component of the distorted supply voltage at PCC. The resulting synchronization phases and frequency are then employed to create the reference axis in the dq-frames. Using (12), where the Park transformation matrix is used, we can determine how to collect the reference voltage signal in dq-frames when only two phases are considered. Furthermore, the Clarke-matrix Equation (13) is used to translate the three-phase load voltage, VL,bc, from the abc-domain to the 0 domain. Then, using Park-matrix and factoring in synchronization phases and frequency from STF- UVG to create the reference axis in the dq-frames,

Indo-American Journal of Agricultural and Veterinary Sciences

ISSN 2321–9602 www.iajavs.com

the 0-domain load voltage signal is transformed to the dq-frames, as shown in (13).

$$\begin{bmatrix} V_{L_\alpha} \\ V_{L_\beta} \\ V_{L_0} \end{bmatrix} = \sqrt{\frac{2}{3}} \begin{bmatrix} 1 & -\frac{1}{2} & -\frac{1}{2} \\ 0 & \frac{\sqrt{3}}{2} & -\frac{\sqrt{3}}{2} \\ \frac{1}{2} & \frac{1}{2} & \frac{1}{2} \end{bmatrix} \begin{bmatrix} V_{L_a} \\ V_{L_b} \\ V_{L_c} \end{bmatrix} \quad (12)$$

$$\begin{bmatrix} V_{L_d} \\ V_{L_q} \end{bmatrix} = \begin{bmatrix} \cos(\omega t) & \sin(\omega t) \\ -\sin(\omega t) & \cos(\omega t) \end{bmatrix} \begin{bmatrix} V_{L_\alpha} \\ V_{L_\beta} \end{bmatrix} \quad (13)$$

Then, the three-phase supply voltage Vs,bc is transformed from the abc-domain to the 0-domain with the help of Clarke-matrix and Equation (14). After that, the reference axis in the dq-frames is

generated from the supply voltage signal in the 0-domain using Park-matrix, taking into account the synchronization phases and frequency from STF-UVG (15).

$$\begin{bmatrix} V_{S_\alpha} \\ V_{S_\beta} \\ V_{S_0} \end{bmatrix} = \sqrt{\frac{2}{3}} \begin{bmatrix} 1 & -\frac{1}{2} & -\frac{1}{2} \\ 0 & \frac{\sqrt{3}}{2} & -\frac{\sqrt{3}}{2} \\ \frac{1}{2} & \frac{1}{2} & \frac{1}{2} \end{bmatrix} \begin{bmatrix} V_{S_a} \\ V_{S_b} \\ V_{S_c} \end{bmatrix} \quad (14)$$

$$\begin{bmatrix} V_{S_d} \\ V_{S_q} \end{bmatrix} = \begin{bmatrix} \cos(\omega t) & \sin(\omega t) \\ -\sin(\omega t) & \cos(\omega t) \end{bmatrix} \begin{bmatrix} V_{S_\alpha} \\ V_{S_\beta} \end{bmatrix} \quad (15)$$

The actual voltage error of the series compensator is calculated by comparing the load voltage, VL,dq, to the supply voltage, Vs,dq, at the power conditioning center (PCC), both in the dq frames. Afterwards, the supply voltage, Vs,dq, at PCC is compared with the reference voltage signal, Vref,dq that is already in phase with supply voltage to determine the accurate reference voltage of the series compensator, which is also measured in the dq frames. The injection reference voltage, VSE,dq, may be found by comparing the nominal reference voltage to the voltage error produced by the series compensator. The proof of the equation may be found in (16), and (17)

$$V_{SE_d}{}^* = \left(V_{ref_d}{}^* - V_{S_d}\right) - \left(V_{L_d} - V_{S_d}\right) \quad (16)$$

$$V_{SE_q}{}^* = \left(V_{ref_q}{}^* - V_{S_q}\right) - \left(V_{L_q} - V_{S_q}\right) \quad (17)$$

Then, Equations (18) and (20) show how the VSE,d and VSE,q may be transformed from dq-frames to the abc-domain (19). Proper gating pulses for the series converter are generated by passing the injection reference voltage series compensator, VSE,abc via a hysteresis voltage controller.

$$\begin{bmatrix} V_{SE_\alpha}{}^* \\ V_{SE_\beta}{}^* \end{bmatrix} = \begin{bmatrix} \sin(\omega t) & \cos(\omega t) \\ -\cos(\omega t) & \sin(\omega t) \end{bmatrix} \begin{bmatrix} V_{SE_d}{}^* \\ V_{SE_q}{}^* \end{bmatrix} \quad (18)$$

$$\begin{bmatrix} V_{SE_a}{}^* \\ V_{SE_b}{}^* \\ V_{SE_c}{}^* \end{bmatrix} = \sqrt{\frac{2}{3}} \begin{bmatrix} 1 & 0 \\ -\frac{1}{2} & \frac{\sqrt{3}}{2} \\ -\frac{1}{2} & -\frac{\sqrt{3}}{2} \end{bmatrix} \begin{bmatrix} V_{SE_\alpha}{}^* \\ V_{SE_\beta}{}^* \end{bmatrix} \quad (19)$$

CONTROL OF SHUNT APF COMPENSATION

The proposed STF on -domain extracts the load current harmonic component. In order to convert the three-phase load current iL,abc from the abc domain to the 0-domain, we use the Clarke-matrix transformation given by the (19). In the -domain, the signal of load current iL, may be decomposed into its fundamental component and its harmonic component. As a result, we may express the connection as (20).

$$\begin{bmatrix} i_{L_\alpha} \\ i_{L_\beta} \\ i_{L_0} \end{bmatrix} = \sqrt{\frac{2}{3}} \begin{bmatrix} 1 & -\frac{1}{2} & -\frac{1}{2} \\ 0 & \frac{\sqrt{3}}{2} & -\frac{\sqrt{3}}{2} \\ \frac{1}{2} & \frac{1}{2} & \frac{1}{2} \end{bmatrix} \begin{bmatrix} i_{L_a} \\ i_{L_b} \\ i_{L_c} \end{bmatrix} \quad (20)$$

$$\begin{bmatrix} i_{L_\alpha} \\ i_{L_\beta} \end{bmatrix} = \begin{bmatrix} i_{L_{\alpha\,(fund)}} + i_{L_{\alpha\,(har)}} \\ i_{L_{\beta\,(fund)}} + i_{L_{\beta\,(har)}} \end{bmatrix} \quad (21)$$

Load current on the -domain has two types of harmonics, the fundamental ones denoted by iL, (fund), and the others by iL, (har). Similarly to the -domain, the -domain represents the load current component as a vector. Load current basic components (iL, (fund)and iL, (fund)on -domainare extracted by Laplace transformation and STF approach, respectively. The equation is shown in (22).

Indo-American Journal of Agricultural and Veterinary Sciences

ISSN 2321–9602 www.iajavs.com

$$\begin{bmatrix} i_{L_{\alpha\,(fund)}}(s) \\ i_{L_{\beta\,(fund)}}(s) \end{bmatrix} = \frac{K_2}{s}\begin{bmatrix} i_{L_\alpha}(s) - i_{L_{\alpha\,(fund)}}(s) \\ i_{L_\beta}(s) - i_{L_{\beta\,(fund)}}(s) \end{bmatrix} + \frac{2\pi f_{c2}}{s}\begin{bmatrix} -i_{L_{\beta\,(fund)}}(s) \\ i_{L_{\alpha\,(fund)}}(s) \end{bmatrix} \quad (22)$$

K2 stands for the constant gain parameter, while fc2 is the cut-off frequency. K2's rating is around 20–80, whereas fc2's rating is frequency– dependent. The anticipated K1 rating for this project is 20, and the fc1 rating is 50 Hz. Theharmonic components (iL, (har) and iL, (har)) may be attained by using the fundamental components (iL, (fund)and iL, (fund)). In (23) we have the calculation:

$$\begin{bmatrix} i_{L_{\alpha\,(har)}} \\ i_{L_{\beta\,(har)}} \end{bmatrix} = \begin{bmatrix} i_{L_\alpha} - i_{L_{\alpha\,(fund)}} \\ i_{L_\beta} - i_{L_{\beta\,(fund)}} \end{bmatrix} \quad (23)$$

The procedure for extracting harmonic components may be seen in Equation (23). The next step is to remove the load current component iL, from the basic components (the STF filter is used for extraction). This necessitates a roundabout approach to extracting the harmonic components. In order to get the harmonic components in d- frame, we utilize the synchronization phases we gotfrom and the harmonic components we got from (6.23). (24).

$$i_{L_{d\,(har)}} = i_{L_{\alpha\,(har)}} \sin(\omega t) - i_{L_{\beta\,(har)}} \cos(\omega t) \quad (24)$$

It is shown in (25) how the initial load current wave in the -domain, iL, and the same synchronized phases may be used to control the transition of the -domain into the frame-q:

$$i_{L_q} = i_{L_\alpha} \cos(\omega t) + i_{L_\beta} \sin(\omega t) \quad (25)$$

To use the 0-domain, a transformation of the 0-domain is unnecessary. The d-steady frame's DC part represents the magnitude of the fundamental load current, while the alternating AC part represents the magnitude of the harmonic current.

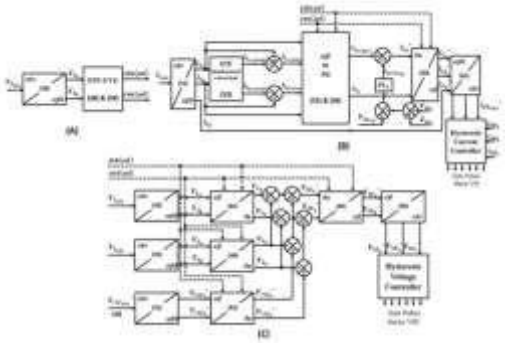

Fig. 6 The UPQC controller scheme's self-tuning filter (STF) block diagram. (A) Shunt-Through-Flux-Gate (STF-UVG); (B) Shunt-Through-Flux-Gate (APF) Control Scheme; (

In addition, the phase information of the load current is stored in the q-frame. Noteworthy is the fact that stabilizing the dc-link voltage necessitates the use of frame-0 of the reference frame dq0, which is directly obtained from the domain-0. Similarly, the unbalanced, harmonic, and reactive currents denoted by the harmonic component of d- frame loads current iL,d (har), the load current iL,q in q-frame, and the load current iL,0, in 0-frame areall unwanted components of load currents. Then, a PI controller is used to bring the difference between the instantaneous total dc-link voltage Vdc,t andthe reference dc-link voltage Vdc,ref down to aknown value, ierror,dc. In (26) and (27), we get the mathematical expression:

$$i_{error_{dc}} = k_{p,4} e_1(t) + k_{i,4} \int_0^t e_1(t)dt \quad (26)$$

$$e_1(t) = V_{dc,ref} - (V_{cap_1}(t) + V_{cap_2}(t)) \quad (27)$$

where the proportional gain and integral gain of the PI4 controller are indicated by the constants kp,4 and ki,4, respectively. In this research, we use the numbers 0.3 and 2 for the variables. Therefore, the current d-frame grid reference is provided in (28):

$$i_{L_d}{}^* = i_{L_{d\,(har)}} - i_{error_{dc}} \quad (28)$$

Then, abc-domain injection reference grid currents are generated using the signals iL,d and iL,q. The standard current iSH,abc is calculated using Equations (29) and (30). The shunt converter gating pulses are generated by a hysteresis current

Indo-American Journal of Agricultural and Veterinary Sciences

ISSN 2321–9602 www.iajavs.com

controller, which compares the injected reference supply currents to the actual supply current.

$$\begin{bmatrix} i_{L_\alpha}^{*} \\ i_{L_\beta}^{*} \end{bmatrix} = \begin{bmatrix} \sin(\omega t) & \cos(\omega t) \\ -\cos(\omega t) & \sin(\omega t) \end{bmatrix} \begin{bmatrix} i_{L_d}^{*} \\ i_{L_q} \end{bmatrix} \quad (29)$$

$$\begin{bmatrix} i_{SH_\alpha}^{*} \\ i_{SH_b}^{*} \\ i_{SH_c}^{*} \end{bmatrix} = \sqrt{\frac{2}{3}} \begin{bmatrix} 1 & 0 \\ -\frac{1}{2} & \frac{\sqrt{3}}{2} \\ -\frac{1}{2} & -\frac{\sqrt{3}}{2} \end{bmatrix} \begin{bmatrix} i_{L_\alpha}^{*} \\ i_{L_\beta}^{*} \end{bmatrix} \quad (30)$$

IV.SIMULATION RESULTS

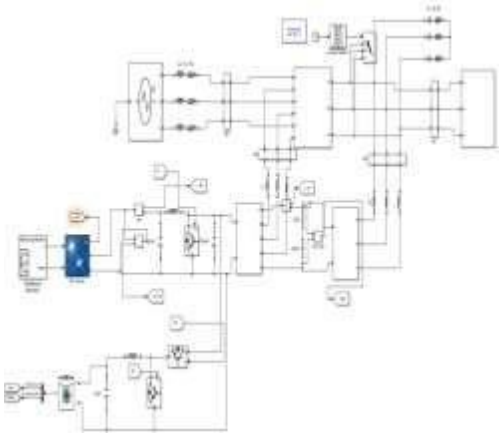

Fig 7 MATLAB/SIMULINK circuit diagram of the system

A. CASE STUDY 1: UPQC USING STF TECHNIQUE CONNECTING EXTERNAL SOURCE OF PV-BESS

1) Scenario A: Balance Harmonic Source Voltage with Non-Linear Load At Constant Irradiance 800 w/m2 at 45°C (Connecting With PV-BESS as External Source of DC-Link)

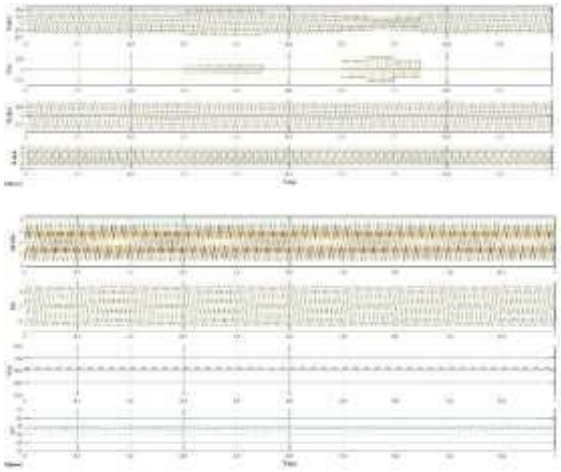

Fig.8 Including (A) three-phase source voltage and (B) injection voltage of Series APF, this is the simulated waveform recorded during Case Study 1 for UPQC connecting with PV-BESS (C) Current (I) at Load Voltage (D) (E) DC link voltage (F), DC link current (G), PV current (F), and Shunt APF injection current (G)

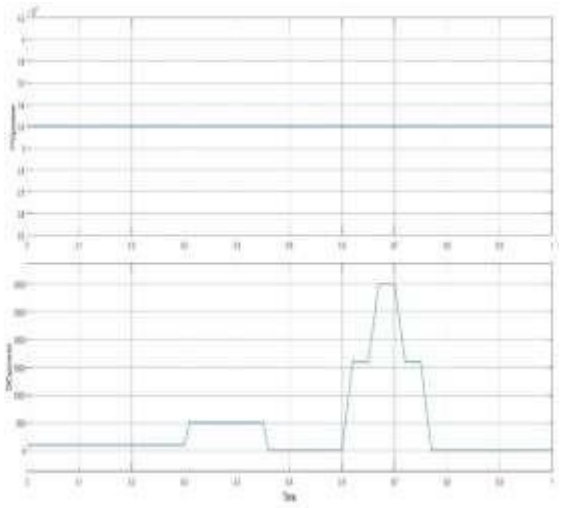

Fig.9 Simulation result acquired under Case Study 1 for UPQC connecting with PV-BESS, with include (A) Power of PV (D) Output power of DC-Link

2) Scenario B: Balance Harmonic Source Voltage with Non-Linear Load At Constant Irradiance 800 w/m2 at 45°C (Without Connecting External Source of PV-BESS)

Indo-American Journal of Agricultural and Veterinary Sciences

ISSN 2321–9602 www.iajavs.com

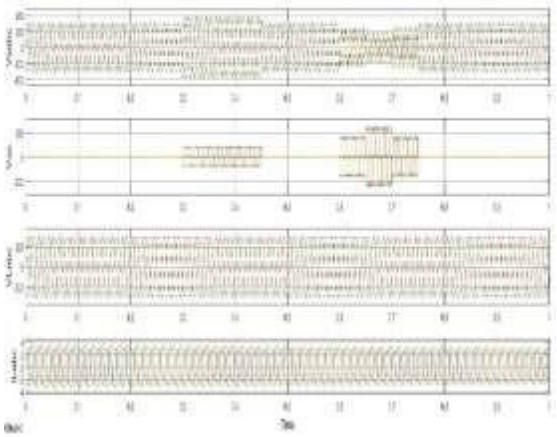

Fig .10 Case Study 1 simulated waveform for UPQC connection without PV-BESS, showing (A) three-phase source voltage (B) injection voltage of Series APF (C) load voltage (D) load current

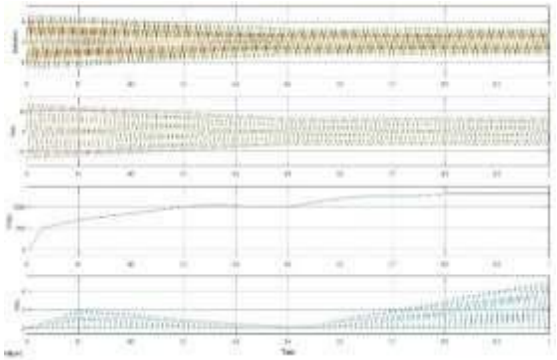

Fig .11 Results from Case Study 1's simulation of UPQC without PV-BESS (A) Shunt APF Current Injection (B) Power Origination (C) Complete Capacitor Voltage (D) The Entire Capacitor Current

B. Case Study 2: Constant PV Irradiance at 800 w/ m2 at 45°C.

1) Scenario A: Sinusoidal-Balance Sag and Swell Source Voltage Condition with Harmonic Non-Linear Load At Constant Irradiance 800 w/m2 at 45°C

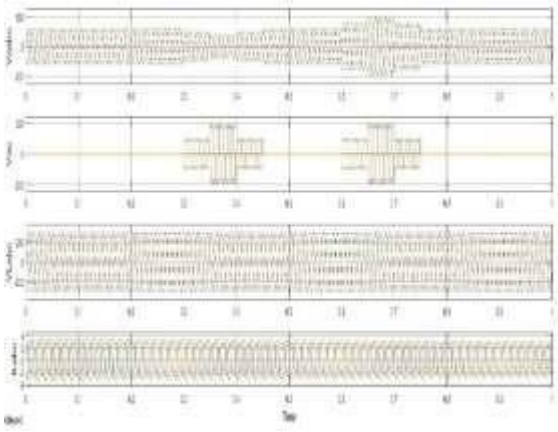

Fig .12 Case Study 2 waveform obtained by simulation: Case Study A: Voltage Swings Up and Down in a Three-Phase Supply with Injection Voltage from a Series APF (C) Amount of Load Current Load Voltage

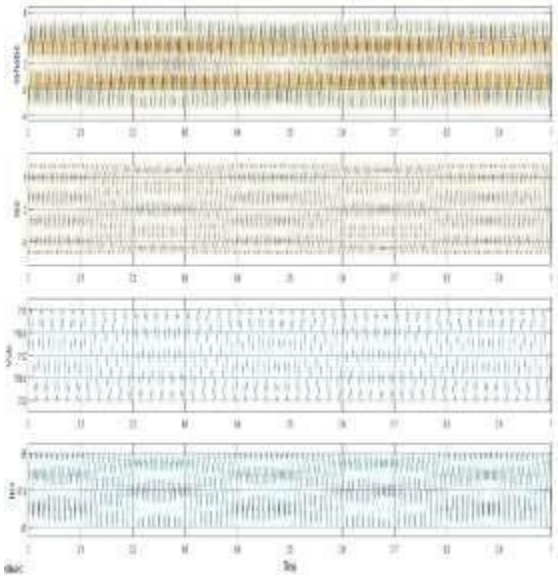

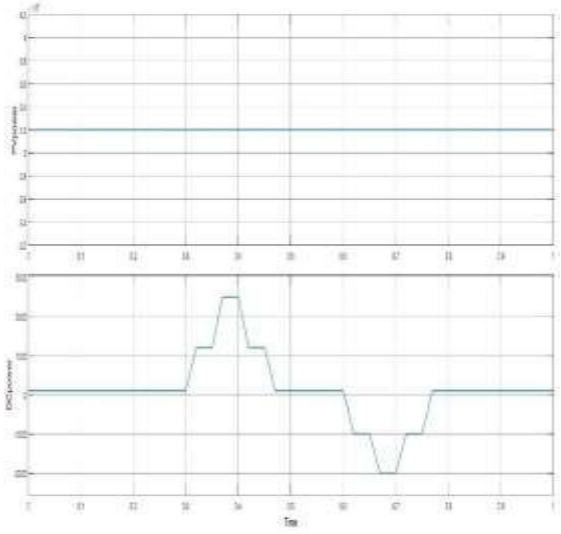

Indo-American Journal of Agricultural and Veterinary Sciences

ISSN 2321–9602 www.iajavs.com

Fig .13 The Case Study 2 simulation results are in: Scenario A: Voltage sag and surge in equilibrium, with shunt APF injection current included (B) DC-Link Source Current (C) Voltage (D) (D) PV Current (E) Energy from PV (F) Strength of DC-Resulting Link's Stream

2) Scenario B: Sinusoidal-Unbalance Sag and Swell Source Voltage Condition with Harmonic Non-Linear Load At Constant Irradiance 800 w/m2 at 45°C

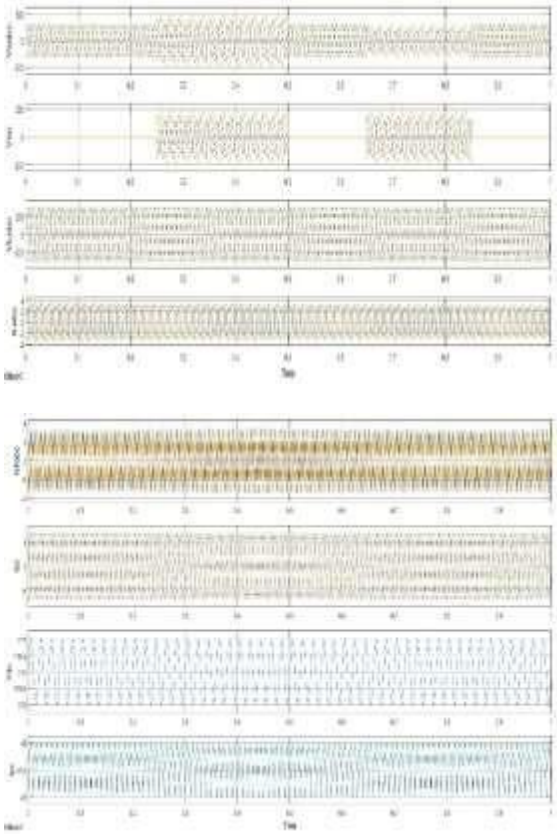

Fig.14 Case Study 2: Scenario B imbalance voltage swell and sag condition simulated waveform, including (A) three-phase source voltage (B) Electron-Pair-Flash (APF) Series Injection Voltage (C) Voltage of the Load (D) Power Draw (E) Shunt APF Current Injection (F) Power Origination (G) AC Current DC Voltage

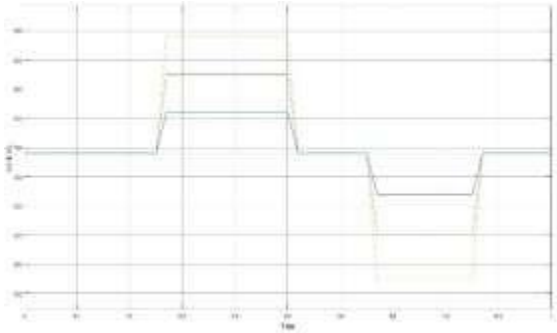

Fig.15 The measured voltage magnitude under Case study 2: Scenario B for an uneven voltage sag and swell situation was collected by simulation.

C. Case Study 3: Varying PV Irradiance and Temperature PV panel.

1) Scenario A: Non-Sinusoidal-unbalance Permanent Interruption Source Voltage with Harmonic Non-Linear Load At Low Unbalance PV Irradiance

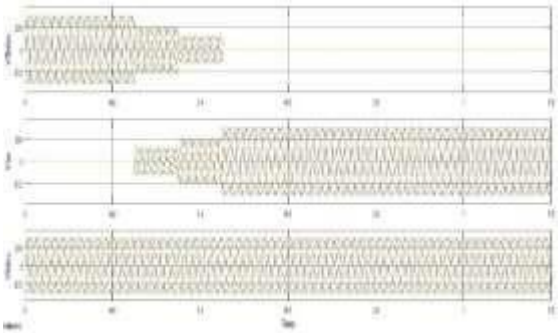

Fig.16 Case Study 3's simulated waveform: Scenario A is a voltage interruption situation, and it consists of the following parts: (A) the three-phase source voltage; (B) the injection voltage of the Series APF; and (C) the load voltage.

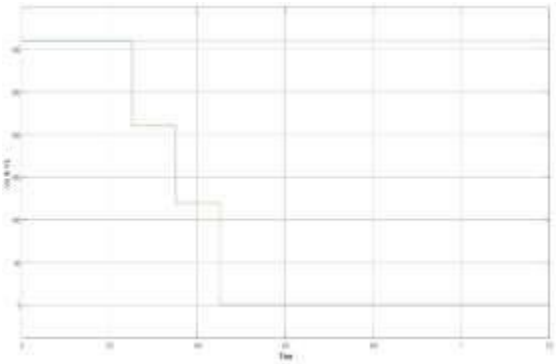

Fig.17 Case Study 3: Scenario A for Voltage Interrupt Condition simulation results obtained the observed voltage magnitude

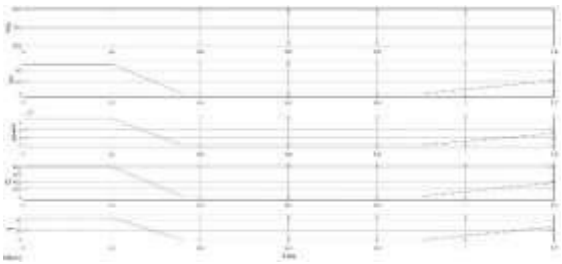

Indo-American Journal of Agricultural and Veterinary Sciences

ISSN 2321–9602 www.iajavs.com

Fig.18 Case Study 2 Scenario A Voltage Interruption Condition Simulation Output, Including (A) DC-Link Voltage (B) PV Current (C) Solar photovoltaic (C) power (D) irradiance (E) temperature

CONCLUSION

In light of the fact that unbalanced and distorted voltage grid conditions contribute to a wide variety of power quality issues, research has been conducted into the design and implementation of three-phase UPQC. The network is given activepower capacity by the combination of the BESS and PV with the UPQC. The primary advantage of a system that combines BESS with UPQC is that it can both provide and absorb active power from PV. Since renewable energy is somewhat reliant on the surrounding environment, a BESS may be used to make up for the unreliability of this source of power. To sum up, it can be deduced that the BESSand PV coupled with UPQC might be a suitable option in the distributed generation to improve the power quality of the modern distribution system. Having a constant supply from the PV-BESS system has allowed for a consistent DC-link voltage. Therefore, it may simplify the algorithm used to control the voltage in the DC connection. In order to provide a stable reference current and voltage, the shunt and series APF compensator implements the STF-UVG approach for synchronization phases. To maintain systemstability and reach almost unity power factor, the UPQC is developed independently of the PLL components, and effective mitigation of current and voltage is accomplished in accordance with the grid state. The harmonics of the grid current have been measured and found to conform to the IEEE-519 standard after the suggested method was put into practice. It's also important to note that the suggested approach has the potential to increasegrid efficiency as a whole.

REFERENCES

[1] Y. Yang, P. Enjeti, F. Blaabjerg, and H. Wang, "Wide-scale adoption of photovoltaic energy: Grid code modifications are explored in the distribution grid," IEEE Ind. Appl. Mag., vol. 21, no. 5, pp. 21–31, Sept 2015.

[2] B. Singh, A. Chandra and K. A. Haddad, Power Quality: Problems and Mitigation Techniques. London: Wiley, 2015.

[3] M. Bollen and I. Guo, Signal Processing of Power Quality Disturbances. Hoboken: Johm Wiley, 2006.

[4] P. Jayaprakash, B. Singh, D. Kothari, A. Chandra, and K. Al-Haddad, "Control of reduced-rating dynamic voltage restorer with a battery energy storage system," IEEE Trans. Ind. Appl., vol. 50, no. 2, pp. 1295– 1303, March 2014.

[5] M. Badoni, A. Singh, and B. Singh, "Variable forgetting factor recursive least square control algorithm for DSTATCOM," IEEE Trans. Power Del., vol. 30, no. 5, pp. 2353–2361, Oct 2015.

[6] A. Rauf and V. Khadkikar, "An enhanced voltage sag compensation scheme for dynamic voltage restorer," IEEE Trans. Ind. Electron., vol. 62, no. 5, pp. 2683–2692, May 2015. [7] V. Khadkikar, "Enhancing electric power quality using UPQC: A comprehensive overview," IEEE Trans. Power Electron., vol. 27, no. 5, pp. 2284–2297, May 2012.

[8] B. Han, B. Bae, H. Kim, and S. Baek, "Combined operation of unified power-quality conditioner with distributed generation," IEEE Trans. Power Del., vol. 21, no. 1, pp. 330–338, Jan 2006.

[9] C. Kumar and M. K. Mishra, "Operation and Control of an Improved Performance Interactive DSTATCOM," IEEE Trans. Ind. Electron., vol. 62, no. 10, pp. 6024–6034, 2015.

[10] Y. Hoon, M. A. M. Radzi, M. K. Hassan, and N. F. Mailah, "Control algorithms of shunt active power filter for harmonics mitigation: A review," Energies, vol. 10, no. 12, 2017.

[11] L. B. Garcia Campanhol, S. A. Oliveira da Silva, and A. Goedtel, "Application of shunt active power filter for harmonic reduction and reactive power compensation in threephase four-wire systems," IET Power Electron., vol. 7, no. 11, pp. 2825–2836, 2014.

[12] Y. Hoon, M. A. M. Radzi, M. K. Hassan, and N. F. Mailah, "Operation of Three-Level Inverter-

Indo-American Journal of Agricultural and Veterinary Sciences

ISSN 2321–9602 www.iajavs.com

Based Shunt Active Power Filter under Nonideal Grid Voltage Conditions with Dual Fundamental Component Extraction," IEEE Trans. Power Electron., vol. 33, no. 9, pp. 7558–7570, 2018.

[13] E. Hossain, M. R. Tur, S. Padmanaban, S. Ay, and I. Khan, "Analysis and Mitigation of Power Quality Issues in Distributed Generation Systems Using Custom Power Devices," IEEE Access, vol. 6, no. c, pp. 16816–16833, 2018.

[14] H. Fujita and H. Akagi, "The unified power quality conditioner: The integration of series- and shunt-active filters," IEEE Trans. Power Electron., vol. 13, no. 2, pp. 315–322, 1998.

[15] S. K. Khadem, M. Basu, and M. F. Conlon, "Intelligent islanding and seamless reconnection technique for microgrid with UPQC," IEEE J. Emerg. Sel. Top. Power Electron., vol. 3, no. 2, pp. 483–492, 2015.

[16] J. M. Guerrero, P. C. Loh, T. L. Lee, and M. Chandorkar, "Advanced control architectures for intelligent microgridsPart II: Power quality, energy storage, and AC/DC microgrids," IEEE Trans. Ind. Electron., vol. 60, no. 4, pp. 1263–1270, 2013.

[17] B. Han, B. Bae, H. Kim, and S. Baek, "Combined operation of unified power-quality conditioner with distributed generation," IEEE Trans. Power Deliv., vol. 21, no. 1, pp. 330–338, 2006.

[18] K. Hasan, M. M. Othman, N. F. A. Rahman, M. A. Hannan, and I. Musirin, "Significant implication of unified power quality conditioner in power quality problems mitigation," Int. J. Power Electron. Drive Syst., vol. 10, no. 4, p. 2231, 2019.

[19] C. K. Sundarabalan, Y. Puttagunta, and V. Vignesh, "Fuel cell integrated unified power quality conditioner for voltage and current reparation in four-wire distribution grid," IET Smart Grid, vol. 2, no. 1, pp. 60–68, 2019.

[20] S. Devassy and B. Singh, "Design and Performance Analysis of Three-Phase Solar PV Integrated UPQC," IEEE Trans. Ind. Appl., vol. 54, no. 1, pp. 73–81, 2018.